



CO₂ emission optimization for a blast furnace considering plastic injection

Xiong Liu^{1,2,3}, Xiaoyong Qin^{1,2,3}, Lingen Chen^{1,2,3}, Fengrui Sun^{1,2,3}

¹ Institute of Thermal Science and Power Engineering, Naval University of Engineering, Wuhan 430033, P. R. China.

² Military Key Laboratory for Naval Ship Power Engineering, Naval University of Engineering, Wuhan 430033, P. R. China.

³ College of Power Engineering, Naval University of Engineering, Wuhan 430033, P. R. China.

Abstract

An optimization model based on mass balance and energy balance for a blast furnace process is established by using a nonlinear programming method. The model takes the minimum CO₂ emission of a blast furnace as optimization objective function, and takes plastic injection or pulverized coal injection into account. The model includes sixteen optimal design variables, six linear equality constraints, one linear inequality constraint, six nonlinear equality constraints, one nonlinear inequality constraint, and thirteen upper and lower bound constraints of optimal design variables. The optimization results are obtained by using the Sequential Quadratic Programming (SQP) method. Comparative analyses for the effects of plastic injection and pulverized coal injection on the CO₂ emission of a blast furnace are performed.

Copyright © 2015 International Energy and Environment Foundation - All rights reserved.

Keywords: Blast furnace; CO₂ emission; Iron-making; Plastic injection; Optimization.

1. Introduction

The iron and steel industry is one of the higher industrial CO₂ emission sources and energy consumers. Around the world, between 4% and 7% of the anthropogenic CO₂ emissions originate from this industry [1-3]. Blast furnace iron-making is a vital process in integrated iron and steel works. The technical improvement and process optimization of blast furnace iron-making is a key step to the development of the iron and steel industry, energy conservation and CO₂ emission reductions [4, 5]. A blast furnace, however, is a reactor containing many very complex physical and chemical processes. Mathematical modeling is an efficient way to obtain further understanding of blast furnace process, and can achieve further improvements of the operations. Currently, some scholars have established different kinds of models for blast furnaces. The models for blast furnace may approximately be divided into three classes: Statistical models [6, 7], kinetic models [8-10] and mass and energy balance models [11-19]. The mass and energy balance model, which is based on thermodynamic theory and takes the characteristics of blast furnace into account, is an effective method to conduct macro analyses and calculations for blast furnace performance. Rasul *et al* [11] established an model for a blast furnace based on mass and energy balances, and analyzed the influences of blast temperature, silicon content in hot metal and ash content in coke on the blast furnace performance. Emre *et al* [12] established a model for a blast furnace based on

the first law of thermodynamics, and analyzed the energy balance of Erdemir No.1 blast furnace. Ziebig *et al* [13, 14] established exergy analysis models for a blast furnace based on mass and energy balances, and analyzed the effects of the operation parameters such as blast temperature and oxygen enrichment degree on exergy and exergy loss of the blast furnace.

In addition, based on mass and energy balances, some optimization models for blast furnace iron-making have been established by using mathematical programming method. Helle *et al* [15] established an optimization model of iron-making process using a linear programming method with biomass as an auxiliary reductant in the blast furnace, and investigated the economy of biomass injection and its dependence on the price structure of materials and emissions. Helle *et al* [16] established a blast furnace iron-making optimization model using nonlinear programming method by taking production as objective function on the basis of the given production rate of hot metal, and analyzed the optimum performance of iron-making system including a blast furnace. Yang *et al* [17] established an optimization model for a blast furnace using linear programming method by taking coke rate as objective function, and proposed some guidelines for the operation of a blast furnace after comparing the optimization result with production reality. Zhang *et al* [18] established a multi-objective optimization model of blast furnace iron-making system using linear programming method by taking energy consumption, cost and CO₂ emissions as objective functions, and analyzed the effects of coke rate, coal rate, blast temperature and sinter ore grade on the energy consumption and cost of production.

The plastic is mainly composed of carbon and hydrogen, and its composition is similar to heavy oil. Thus, the application value of plastic for blast furnace smelting is obvious. To a certain extent, the technology of injecting plastic into a blast furnace can solve environmental problem caused by the extensive use of plastic. Hence, the industrial application value and environmental protection value of plastic injection in blast furnace have been noted by researchers [19-21]. Minoru *et al* [19] described the development of waste plastics injection for blast furnaces. Dongsu *et al* [20] conducted an experiment on plastic injection for blast furnaces and discovered that the combustion efficiency of plastic in tuyere zone could be improved by improving blast temperature and oxygen enrichment degree, and reducing plastic particle size. Minor *et al* [21] conducted experiments on plastic injection in blast furnaces and found that the combustion performance of plastic in a blast furnace is equivalent to pulverized coal when a plastic particle is less than 1.44 mm.

Based on the studies mentioned above, a blast furnace optimization model, in which CO₂ emissions of the blast furnace is taken as an objective function, is established, and the plastic injection and pulverized coal injection are considered. Then, the model is solved by using the Sequential Quadratic Programming (SQP) method from MATLAB optimization toolbox. In addition, the effects of plastic injection and pulverized coal injection on the CO₂ emissions of a blast furnace are analyzed and contrasted. The conclusions obtained herein can provide some guidelines for the design and operation of blast furnaces.

2. The CO₂ emission optimization model for a blast furnace

2.1 Physical model

As shown in Figure 1, a physical model of a blast furnace is considered based on the temperature characteristics inside the blast furnace and some division methods proposed in Refs. [22, 23]. The blast furnace is divided into three zones along its height: the upper preparation zone (PZ), the middle reserve zone (RZ) and the bottom elaboration zone (EZ). The inputs of material flows include sinter ore, pellet ore, lump ore, coke, blast and fuel injected into tuyere area. The outputs of material flows include hot metal, slag and blast furnace gas. The limit temperature of the bottom elaboration zone is set as 950 °C; the middle reserve zone is considered as an isothermal region of 950 °C, and the upper preparation zone is a lumpish zone while its temperature is lower than 950 °C. Furthermore, the following assumptions are considered: (1) All the high valence iron oxides in the preparation zone are reduced into wustite; (2) The gasification of carbon only takes place in the elaboration zone; (3) Behaviors in a blast furnace are described according to the theory of Rist operation; (4) The combustion efficiency of fuel in blast furnace is 100%; (5) Both free water and crystal water in raw material and fuel are evaporated or separated in the preparation zone.

The chemical reaction relations exist in the elaboration zone are listed in Table 1.

The main chemical reactions present in the middle reserve zone are: indirect reduction of wustite ($\text{FeO} + \text{CO} = \text{Fe} + \text{CO}_2$) and water gas shift reaction ($\text{CO} + \text{H}_2\text{O} = \text{CO}_2 + \text{H}_2$).

The main chemical reactions present in the preparation zone are: decomposition of carbonate (excluding flux); both the free water and crystal water of raw material and fuel are evaporated or separated; carbon deposition ($2\text{CO} = \text{CO}_2 + \text{C}$); hematite and magnetite are completely reduced to wustite.

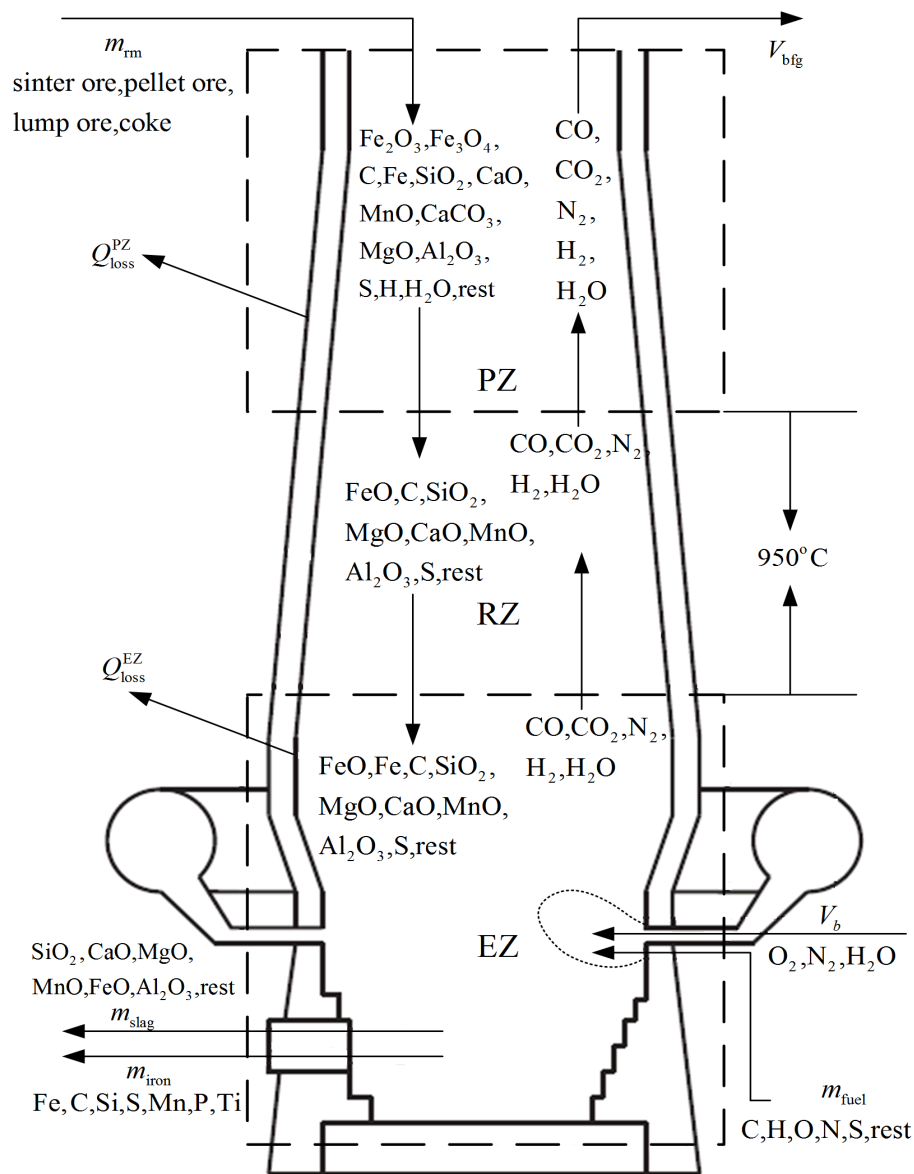


Figure 1. Physical model of a blast furnace

Table 1. Chemical reactions and their introductions in the elaboration zone

chemical reaction	introduction
$\text{FeO} + \text{C} = \text{Fe} + \text{CO}$	direct reduction of wustite
$\text{SiO}_2 + 2\text{C} = \text{Si} + 2\text{CO}$	direct reduction of SiO_2
$\text{MnO} + \text{C} = \text{Mn} + \text{CO}$	direct reduction of MnO
$\text{P}_2\text{O}_5 + 5\text{C} = 2\text{P} + 5\text{CO}$	direct reduction of P_2O_5
$\text{FeS} + \text{CaO} + \text{C} = \text{CaS} + \text{Fe} + \text{CO}$	desulfurization
$\text{C} + \text{O}_2 = 2\text{CO}$	combustion of carbon
$\text{CO}_2 + \text{C} = 2\text{CO} (>1000^{\circ}\text{C})$	reduction of CO_2
$\text{C} + \text{H}_2\text{O} = \text{CO} + \text{H}_2 (>1000^{\circ}\text{C})$	reduction of water in blast

2.2 Optimal design variables

The performance of a blast furnace is affected by many factors. These factors include three classes: (1) raw material and fuel parameters, (2) process parameters and (3) product quality parameters. The raw material parameters refer to the dosage of iron ore and flux. The fuel parameters refer to the coke rate and injected fuel rate. The process parameters refer to the direct reduction degree of iron, blast parameters (including volume, temperature, humidity and oxygen enrichment degree), slag basicity, volume of blast furnace gas and coke load. The product quality parameters refer to the content of each ingredient in hot metal.

Some main techno-economic indexes of iron-making process are often influenced by these parameters. Thus, as listed in Table 2, sixteen parameters are chosen from these three kinds of parameters as optimal design variables.

Table 2. Optimal design variables and introductions

parameter categories	variables	symbols	units	introductions
raw material parameters	X ₁	m_{sinter}	kg/t	sinter ore rate
	X ₂	m_{pellet}	kg/t	pellet ore rate
	X ₃	m_{lump}	kg/t	lump ore rate
	X ₄	m_{is}	kg/t	flux rate
fuel parameters	X ₅	$m_{\text{fuel, injected}}$	kg/t	injected fuel rate
	X ₆	m_{coke}	kg/t	coke rate
technological parameters	X ₇	r_d	-	direct reduction degree of iron
	X ₈	V_b	Nm ³ /t	blast volume
	X ₉	T_b	°C	blast temperature
	X ₁₀	φ	%	blast humidity
	X ₁₁	f	%	blast oxygen enrichment degree
quality parameters of production	X ₁₂	[Fe]	%	Fe content in hot metal
	X ₁₃	[C]	%	C content in hot metal
	X ₁₄	[P]	%	P content in hot metal
	X ₁₅	[Mn]	%	Mn content in hot metal
	X ₁₆	[S]	%	S content in hot metal

2.3 Objective function

In fact, there are various carbon gases in the blast furnace gas. Thus, the CO₂ emissions value should be the mass of all the CO₂ when the carbon gases are converted to CO₂ [24]. According to this method of calculation on CO₂ emissions, and the carbon gas in blast furnace is composed of CO and CO₂, the CO₂ emission objective function is expressed as

$$F = \frac{44V_{\text{bfg}} \cdot (\omega_{\text{CO}_2, \text{bfg}} + \omega_{\text{CO}, \text{bfg}})}{2.24} \text{ (kg/t)} \quad (1)$$

where V_{bfg} is the blast furnace gas volume (Nm³/t), $\omega_{\text{CO}, \text{bfg}}$ is the volume content of CO within blast furnace gas (%), and $\omega_{\text{CO}_2, \text{bfg}}$ is the volume content of CO₂ within blast furnace gas (%).

2.4 Constraint conditions

The process of blast furnace iron-making must obey the laws of mass and energy balances, and also needs to conform to a certain process system and some material conditions. Thus, all the constraint conditions are classified into mass and energy balance constraints, process constraints, and upper and lower bound constraints of the optimal design variables.

2.4.1 Mass and energy balance constraints

Mass and energy balance constraints include hot metal composition balance constraint, ferrum element balance constraint, manganese element balance constraint, phosphorus element balance constraint, sulfur

element balance constraint, dissolved carbon balance constraint, heat balance constraint for the elaboration zone, and carbon and oxygen balance constraints for the elaboration zone.

The hot metal composition balance constraint for blast furnace means that the sum of the contents of each kind of element in hot metal is 100%, so its constraint function is

$$\sum [j] = 100 \quad (2)$$

where $[j]$ is the content of each kind of element in hot metal (%).

The balance constraints of ferrum element, manganese element, phosphorus element and sulfur element mean that the inputs of each kind element within a blast furnace should be equal to the outputs of it. Thus, the constraint function is

$$\sum (m_i \cdot \omega_{i,j} / 100) = 10[j] \text{ (kg/t)} \quad (3)$$

where m_i is the dosage of each kind of raw material and fuel (kg/t), and $\omega_{i,j}$ is the content of element j (Fe, P, Mn, S) in each kind of raw material and fuel (%).

The dissolved carbon balance constraint means that the carbon content of hot metal has a relationship with the other element content within the hot metal. As it is hard to control the content of carbon in hot metal, the corrected formula is adopted in this model according to Ref. [25]:

$$[C] = 4.3 - 0.27[Si] - 0.32[P] - 0.032[S] + 0.03[Mn] \text{ (%) } \quad (4)$$

The heat balance constraint in the elaboration zone means that the heat inputs should be equal to the heat outputs in the elaboration zone [26]. Thus, its constraint function is

$$Q_c + Q_b + Q_{\text{fuel}} = Q_{\text{df}} + Q_{\text{dr}} + Q_{\text{dcar}} + Q_{\text{bfg}} + Q_{\text{iron}} + Q_{\text{slag}} + Q_{\text{loss}}^{\text{EZ}} \text{ (kJ/t)} \quad (5)$$

where Q_c , Q_b and Q_{fuel} are, respectively, heat release of carbon combustion, physical heat of blast (excluding decomposition heat of water in blast) and physical heat of injected fuel (kJ/kg); Q_{df} , Q_{dr} , Q_{dcar} , Q_{bfg} , Q_{iron} , Q_{slag} and $Q_{\text{loss}}^{\text{EZ}}$ are, respectively, decomposition heat of injected fuel, demanded heat of direct reduction of ferrum element and other alloying elements, decomposition heat of carbonate, physical heat of blast furnace gas, physical heat of hot metal, physical heat of slag, and heat loss of the elaboration zone (kJ/kg).

When the blast furnace iron-making process is in equilibrium state, the coke rate from calculation is the lowest coke rate, namely theoretical coke rate [25]. Actually, because the blast furnace iron-making process is always in a non-equilibrium state, the constraint function of carbon oxygen balance for the elaboration zone is

$$10[Fe]/56 \cdot \eta_{\text{H}_2} \cdot V_{\text{H}_2,r} / 0.0224 - (m_{\text{C,b}} + m_{\text{C,da}} + m_{\text{C,dFe}} - 10[C]) / 12 / 3.237 \leq m_{\text{C,dFe}} / 12 \quad (6)$$

where η_{H_2} is the hydrogen utilization ratio, $V_{\text{H}_2,r}$ is the volume of hydrogen involved in reduction reaction, $m_{\text{C,b}}$, $m_{\text{C,da}}$ and $m_{\text{C,dFe}}$ are, respectively, the mass of carbon burning in raceway, the mass of carbon involved in direct reduction for alloying elements (including the mass of carbon involved in solution loss reaction and desulfurization), and the mass of carbon involved in direct reduction for iron.

2.4.2 Process constraints

Process constraints include constraint of slag basicity, constraint of the content of MgO in slag, constraint of the content of Al_2O_3 in slag, constraint of coke load, constraint of sulfur load, constraint of blast temperature, constraint of oxygen enrichment degree, constraint of blast humidity, and constraint of the relationship between hydrogen utilization ratio and carbon monoxide utilization ratio. These constraints are listed in Table 3.

Table 3. Process constraints and constraint functions

process constraints	constraint functions
constraint of slag basicity (R)	$R_{\min} \leq R \leq R_{\max}$
content constraint of MgO in slag ($\omega_{\text{MgO,slag}}$)	$\omega_{\text{MgO,slag}} = \sum \omega_{\text{MgO}_i} \cdot m_i / m_{\text{slag}}$
content constraint of Al_2O_3 in slag ($\omega_{\text{Al}_2\text{O}_3,\text{slag}}$)	$\omega_{\text{Al}_2\text{O}_3,\text{slag}} \leq \omega_{\text{Al}_2\text{O}_3,\text{slag,max}}$
constraint of coke load (L_{coke})	$L_{\text{coke,min}} \leq L_{\text{coke}} \leq L_{\text{coke,max}}$
constraint of sulfur load (L_{S})	$L_{\text{S}} \leq L_{\text{S,max}}$
constraint of blast temperature (t_{b})	$t_{\text{b,min}} \leq t_{\text{b}} \leq t_{\text{b,max}}$
constraint of oxygen enrichment degree (f)	$f_{\min} \leq f \leq f_{\max}$
constraint of blast humidity (φ)	$\varphi_{\min} \leq \varphi \leq \varphi_{\max}$
constraint of the relationship between hydrogen utilization ratio and carbon monoxide utilization ratio (η_{H_2})	$\eta_{\text{H}_2} = 0.88 \times \omega_{\text{CO}_2,\text{bfg}} \cdot (\omega_{\text{CO},\text{bfg}} + \omega_{\text{CO}_2,\text{bfg}}) + 0.1$

2.4.3 Upper and lower bound constraints for optimal design variables

All of the optimal design variables in the model come from raw material parameters, fuel parameters, process parameters and product quality parameters. These optimal design variables should be within the allowable ranges. In addition, as blast temperature, oxygen enrichment degree of blast and blast humidity have been contained in process constraints, the upper and lower bounds of the other thirteen optimal design variables needed to be given. The constraint functions of upper and lower bound of the optimal design variables can be written as

$$\text{lb}_i \leq x_i \leq \text{ub}_i \quad (7)$$

where x_i is optimal design variable, lb_i and ub_i are, respectively, upper and lower bounds of optimal design variables.

3. Description of the optimization problem and its solution

3.1 Description of the optimization problem

The optimization problem in this model is a nonlinear programming problem with multivariable and multi-dimensional constraints [27]. Its mathematical description can be expressed as follows:

$$\left\{ \begin{array}{l} \min \quad f(x) \\ \text{s.t.} \quad c(x) \leq 0 \\ \quad \quad c_{\text{eq}}(x) = 0 \\ \quad \quad Ax \leq b \\ \quad \quad A_{\text{eq}}x = b_{\text{eq}} \\ \quad \quad \text{lb} \leq x \leq \text{ub} \end{array} \right. \quad (8)$$

where $f(x)$ is objective function, x , b , b_{eq} and lb are, respectively, n dimension column vector, m_1 dimension column vector, and m_2 dimension column vector. $c(x)$ and $c_{\text{eq}}(x)$ are, respectively, nonlinear functions of return vectors, ub and lb are, respectively, upper and lower bounds of optimal design variables, while both ub and lb have the same dimension with x .

3.2 Solutions of constraint conditions and objective function

In order to obtain the values of constraint conditions and objective function, the results of material balance calculation and heat balance calculation should be substituted into constraint conditions and objective function, when the initial values of the optimal design variables are given. Thus, at first, it is necessary to calculate the material and heat balances [26].

3.2.1 Material balance calculation

The material balance calculation includes calculation of slag mass and its composition contents, blast volume, blast furnace gas volume and its composition contents.

The calculation methods of slag mass and its composition contents are listed in Table 4.

The blast volume V_b is

$$V_b = \frac{22.4m_b}{24\varphi_{O_2,b}} (\text{Nm}^3/\text{t}) \quad (9)$$

where m_b is the mass of carbon burned in the raceway (kg/t), and $\varphi_{O_2,b}$ is the content of oxygen in the blast air.

Blast furnace gas is composed of H_2 , CO_2 , CO and N_2 . The calculation methods of blast furnace gas volume and its composition contents are listed in Table 5.

Table 4. Calculation of slag mass and its composition content*

symbol	introduction	unit	calculation method
$m_{SiO_2,slag}$	SiO ₂ mass in slag	kg/t	$m_{SiO_2,slag} = \sum \omega_{SiO_2,i} \cdot m_i / 100 - 10[Si] \times 30 / 28$
$m_{CaO,slag}$	CaO mass in slag	kg/t	$m_{CaO,slag} = \sum \omega_{CaO,i} \cdot m_i / 100$
$m_{MgO,slag}$	MgO mass in slag	kg/t	$m_{MgO,slag} = \sum \omega_{MgO,i} \cdot m_i$
$m_{Al_2O_3,slag}$	Al ₂ O ₃ mass in slag	kg/t	$m_{Al_2O_3,slag} = \sum \omega_{Al_2O_3,i} \cdot m_i$
$m_{FeO,slag}$	FeO mass in slag	kg/t	$m_{FeO,slag} = \sum (\omega_{TFe,i} \cdot m_i \cdot \eta_{Fe,slag}) \times 72 / 56 / 100$
$m_{Mn,slag}$	Mg mass in slag	kg/t	$m_{Mn,slag} = \sum (\omega_{Mn,i} \cdot m_i \cdot \eta_{Mn,slag}) \times 71 / 55 / 100$
$m_{S,slag}$	S mass in slag	kg/t	$m_{S,slag} = 0.5 \sum (\omega_{S,i} \cdot m_i \cdot \eta_{S,slag}) \times 32 / 100$
m_{slag}	slag mass	kg/t	$m_{slag} = m_{SiO_2,slag} + m_{CaO,slag} + m_{MgO,slag} + m_{Al_2O_3,slag} + m_{FeO,slag} + m_{Mn,slag} + m_{S,slag}$

* $\omega_{SiO_2,i}$, $\omega_{CaO,i}$, $\omega_{MgO,i}$, $\omega_{TFe,i}$, $\omega_{Mn,i}$ and $\omega_{S,i}$ are, respectively, the contents of SiO₂, CaO, MgO, TFe, Mn and S in each kind of raw material (%), i is each kind of raw material, $\eta_{Fe,slag}$, $\eta_{Mn,slag}$ and $\eta_{S,slag}$ respectively are the distribution rate of Fe, Mn and S in slag.

Table 5. Calculation of blast furnace gas volume and its composition content*

symbol	introduction	unit	calculation method
$V_{H_2,bfg}$	volume of H ₂ in blast furnace gas	Nm ³ /t	$V_{H_2,bfg} = (1 - \eta_{H_2}) \cdot (V_{H_2,b} + V_{H_2,fuel})$
$V_{CO,bfg}$	volume of CO in blast furnace gas	Nm ³ /t	$V_{CO,bfg} = V_{CO,b} + V_{CO,d} - V_{CO,id}$
$V_{CO_2,bfg}$	volume of CO ₂ in blast furnace gas	Nm ³ /t	$V_{CO_2,bfg} = V_{CO_2,r} + \sum V_{CO_2,i}$
$V_{N_2,bfg}$	volume of N ₂ in blast furnace gas	Nm ³ /t	$V_{N_2,bfg} = V_{N_2,b} + V_{N_2,fuel}$
V_{bfg}	blast furnace gas volume	Nm ³ /t	$V_{bfg} = V_{H_2,bfg} + V_{CO,bfg} + V_{CO_2,bfg} + V_{N_2,bfg}$

* η_{H_2} is hydrogen utilization rate, $V_{H_2,b}$ is the volume of water in blast (Nm³/t), $V_{H_2,fuel}$ is the volume of H₂ within injected fuel (Nm³/t), $V_{CO,b}$ is the volume of CO produced by the combustion of carbon in raceway (Nm³/t), $V_{CO,d}$ is the volume of CO produced by the direction reduction of iron and other alloying elements (Nm³/t), $V_{CO,id}$ is the volume of CO used by the indirect reduction (Nm³/t), $V_{CO_2,r}$ is the volume of CO₂ produced in reduction reaction (Nm³/t), $V_{CO_2,i}$ is the volume of CO₂ in each kind of raw material (Nm³/t), $V_{N_2,b}$ is the volume of N₂ in blast (Nm³/t), $V_{N_2,fuel}$ is the volume of N₂ in injected fuel (Nm³/t).

3.2.2 Heat balance calculation

Heat inputs of a blast furnace include heat released by combustion of carbon in raceway and physical heat of the hot blast air. Heat outputs of blast furnace include heat demand of reduction reaction, heat

demand of desulfurization, heat demand of carbonate decomposition, physical heat of slag, physical heat of hot metal, physical heat of blast furnace gas, heat demand of evaporation of water in raw materials and heat carried by cooling water and heat loss. The calculation methods of those are listed in Table 6.

Table 6. Calculation of each kind of heat*

	symbol	introduction	unit	calculation method
heat input	$Q_{c,b}$	heat released by combustion of carbon in raceway	kJ/t	$Q_{c,b} = 9781.2m_{c,b} - q_{dm} \cdot m_{fuel}$
	Q_b	physical heat of hot-blast air	kJ/t	$Q_b = V_b \cdot \bar{C}_{p,b} \cdot t_b - 10806(1-f) \cdot \varphi$
heat output	Q_d	heat demand for reduction reaction	kJ/t	$Q_d = 2890 \times 10[Fe] \cdot r_d + 22960 \times 10[Si] + 4880 \times 10[Mn] + 26520 \times 10[P]$
	Q_s	heat demand for desulfurization	kJ/t	$Q_s = 4650\omega_s \cdot m_{slag}$
	Q_{carb}	heat demand for carbonate decomposition	kJ/t	$Q_{carb} = \sum q_{d,i} \cdot m_{carb,i}$
	Q_{slag}	physical heat of slag	kJ/t	$Q_{slag} = m_{slag} \cdot h_{slag,out}$
	Q_{iron}	physical heat of hot metal	kJ/t	$Q_{iron} = 1000h_{iron,out}$
	Q_{bfg}	physical heat of blast furnace gas	kJ/t	$Q_{bfg} = V_{bfg} \cdot C_{bfg} \cdot t_d + V_{H_2O,r} \cdot C_{H_2O} \cdot t_d$
	Q_{H_2O}	heat demand for evaporation of water in raw materials and heat carried out by cooling water	kJ/t	$Q_{H_2O} = 2450 \sum (\omega_{H_2O,i} \cdot m_i / 100)$
	Q_{loss}	heat loss	kJ/t	$Q_{loss} = 10Z_0 \cdot \omega_{C,coke} / \eta_v$

* $m_{c,b}$ is the quantity of carbon burned in raceway (kg/t), q_{dm} is heat demanded for injected fuel decomposition (kJ/t), $\bar{C}_{p,b}$ is the specific heat capacity of blast (kJ/(m³·°C)), f and φ respectively are oxygen enrichment degree and humidity of blast, $m_{carb,i}$ is quantity of carbon within each kind of raw material (kg/t), $q_{d,i}$ is heat demanded for decomposition of carbonate within each kind of raw material (kJ/t), $h_{slag,out}$ is specific enthalphy of slag of hot metal (kJ/kg), C_{bfg} is specific heat capacity of blast furnace gas (kJ/(m³·°C)), t_d is temperature of blast furnace gas (°C), $V_{H_2O,r}$ is volume of water produced by reduction reaction in which hydrogen involved (Nm³/t), C_{H_2O} is the specific heat capacity of water vapor (kJ/(m³·°C)), $\omega_{H_2O,i}$ is the content of water within each kind of raw material and fuel (%), η_v is productivity (kJ/(m³·d)), Z_0 is heat loss of one kilogram carbon when smelting intensity is one (kJ/kgC), $\omega_{C,coke}$ is the content of carbon in coke (%).

3.3 Optimization method

The optimization problem in this model is a nonlinear programming problem with multivariable and multi-dimensional constraints. Its objective function is a nonlinear function. Its constraints include nonlinear equality constraints, nonlinear inequality constraints, linear equality constraints and linear inequality constraints. The function of “fmincon” in the optimization toolbox of the MATLAB is used to find the optimization results of nonlinear programming problem with multivariable and multi-dimensional constraints [27]. As SQP algorithm has global and superlinear convergence, it has been one of the most efficient nonlinear programming algorithms in solving nonlinear programming problem with multivariable and multi-dimensional constraints [28]. Then, the function of “fmincon” in the optimization toolbox of the MATLAB is adopted in this model, and its call form is

$$[x, fval]=fmincon(@objfun,x_0,A,b,Aeq,beq,lb,ub,@confun,options) \tag{10}$$

where x_0 is a initial point, x is optimal solution, and $fval$ is the minimum of the objective function.

4. Optimization results and analyses

A designed blast furnace described in Ref. [26] is taken as an example. The contents of plastic and pulverized coal are listed in Table 7.

Table 7. Contents of plastic and pulverized coal (%)

item	C	S	O	H	N	H ₂ O	FeO	SiO ₂	CaO	MgO	Al ₂ O ₃
plastic	85.60	14.40	-	-	-	-	-	-	-	-	-
pulverized coal	85.40	0.550	0.460	0.300	0.310	0.37	0.847	5.950	0.800	0.710	4.373

The upper and lower bounds of the optimal design variables are listed in Table 8. The upper bound of injected fuel is 170 kg/t-hot metal when pulverized coal is injected. The upper bound of injected fuel is 100 kg/t-hot metal when plastic is injected. The upper and lower bounds of the other optimal design variables with pulverized coal injection are the same as those of optimal design variables with plastic injection.

Table 8. Upper and lower bounds of the optimal design variables

variable	unit	upper bound	lower bound	variable	unit	upper bound	lower bound
x ₁	kg/t	1500	0	x ₉	°C	1250	1050
x ₂	kg/t	1000	0	x ₁₀	%	2.0	0
x ₃	kg/t	158.52	0	x ₁₁	%	6.0	0
x ₄	kg/t	80	0	x ₁₂	%	100	94
x ₅	kg/t	100 (plastic injection) 170 (pulverized coal injection)	0	x ₁₃	%	4.9	0
x ₆	kg/t	500	200	x ₁₄	%	0.4	0
x ₇	-	1	0.3	x ₁₅	%	1.2	0
x ₈	Nm ³ /t	1800	700	x ₁₆	%	0.07	0

4.1 Optimization results

The optimization results and original ones are listed in Table 9. As shown in Table 9, the optimal pulverized coal rate reaches the lower bound (0 kg/t-hot metal) when pulverized coal is injected. In contrast, the optimal plastic rate reaches the upper bound (100 kg/t-hot metal) when plastic is injected.

Table 9. Optimization results and original results

variable	introduction	symbol	unit	optimization results with plastic injection	optimization results with pulverized coal injection	original results
x ₁	sinter ore rate	m_{sinter}	kg/t	840.25	998.23	1030.35
x ₂	pellet ore rate	m_{pellet}	kg/t	575.13	436.12	396.29
x ₃	lump ore rate	m_{lump}	kg/t	158.52	158.52	158.52
x ₄	flux rate	m_{ls}	kg/t	0	0	0
x ₅	injected fuel rate	m_{fuel}	kg/t	100	0	170
x ₆	coke rate	m_{coke}	kg/t	270.86	448.94	325
x ₇	direct reduction degree of iron	r_{d}		0.39	0.56	0.45
x ₈	blast volume	V_{b}	m ³ /t	865.32	1005.32	1000.48
x ₉	blast temperature	T_{b}	°C	1250	1250	1250
x ₁₀	blast humidity	φ	%	0	0	2.0
x ₁₁	blast oxygen enrichment degree	f	%	0	0	3.5
x ₁₂	Fe content in hot metal	[Fe]	%	95.09	95.09	94.34
x ₁₃	C content in hot metal	[C]	%	4.16	4.16	4.90
x ₁₄	P content in hot metal	[P]	%	0.09	0.10	0.10
x ₁₅	Mn content in hot metal	[Mn]	%	0.14	0.13	0.15
x ₁₆	S content in hot metal	[S]	%	0.03	0.03	0.025
-	minimum CO ₂ emissions	-	kg/t	1013.96	1272.44	1344.30

In addition, both blast humidity (φ) and blast oxygen enrichment degree (f) reaches the lower bound whether plastic or pulverized coal is injected. The CO₂ emissions of blast furnace with pulverized coal injection decrease 6.27% after optimization. In fact, the metal oxide content of coal is higher than that of coke, so both heat demand of reduction and carbon dosage with pulverized coal injection are increased. Hence, the mass of pulverized coal reaches 0 kg/t-hot metal when CO₂ emissions of blast furnace reach the minimum. In contrast, the CO₂ emissions of blast furnace are decreased 24.57% with plastic injection. This is due to the fact that plastic contains high hydrogen content and has no metal oxide. Thus, one can conclude that plastic injection will decrease CO₂ emissions of a blast furnace, while pulverized coal injection will increase CO₂ emissions of a blast furnace. While from the perspective of economics, burning coke only is not practical while plastic injection is economical. Thus, plastic injection has significance for both emission reduction and economic considerations.

4.2 Analyses of influence factors

4.2.1 Influence of injected fuel rate on optimization results

Figures 2-5 show the relationships among the minimum CO₂ emission (F_{min}) and the corresponding fuel rate (m_{fuel}), coke rate (m_{coke}), direct reduction degree of iron (r_d) and injected fuel rate ($m_{fuel,injected}$), respectively.

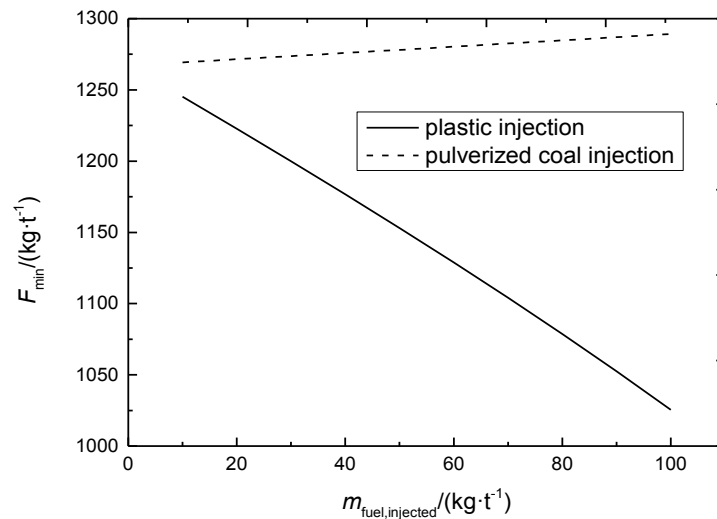


Figure 2. The minimum CO₂ emission (F_{min}) versus injected fuel rate ($m_{fuel,injected}$)

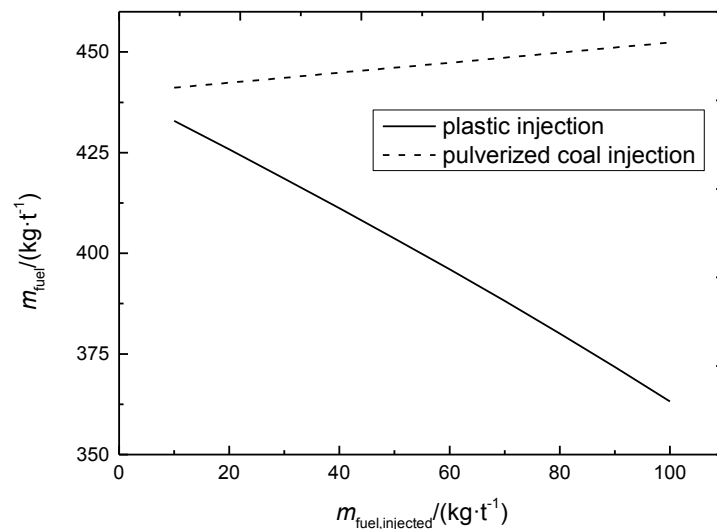


Figure 3. The fuel rate (m_{fuel}) versus injected fuel rate ($m_{fuel,injected}$) corresponding to the minimum CO₂ emission (F_{min})

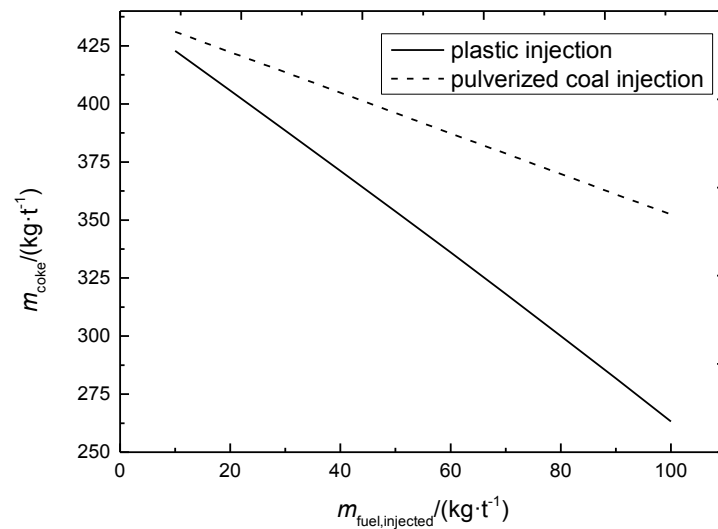


Figure 4. Coke rate (m_{coke}) versus injected fuel rate ($m_{\text{fuel, injected}}$) corresponding to the minimum CO_2 emission (F_{min})

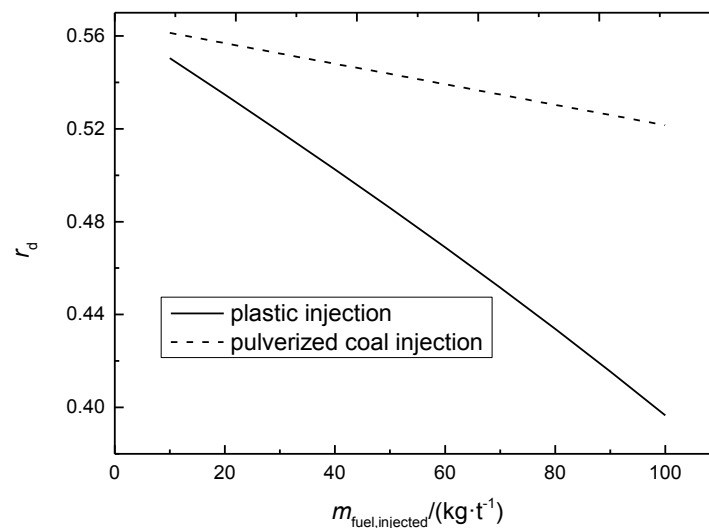


Figure 5. Direct reduction degree of iron (r_d) versus injected fuel rate ($m_{\text{fuel, injected}}$) corresponding to the minimum CO_2 emission (F_{min})

From Figures 2 and 3, one can see that the minimum CO_2 emission (F_{min}) and its corresponding fuel rate (m_{fuel}) decrease when the plastic injection rate (m_{plastic}) increases. In contrast, the minimum CO_2 emission (F_{min}) and its corresponding injected fuel rate ($m_{\text{fuel, injected}}$) increase when pulverized coal rate (m_{coal}) increases. The reason is that the content of hydrogen in plastic is relatively high and the amount of hydrogen takes the place of carbon to take part in reduction, and thus the carbon consumption is decreased. Then, the minimum CO_2 emission (F_{min}) and fuel rate (m_{fuel}) decrease. In contrast, as the content of hydrogen in coal is lower than that in plastic and a certain amount of metal oxide exist in coal, the carbon consumption increases. Then, the minimum CO_2 emission (F_{min}) and fuel rate (m_{fuel}) decrease. From Figures 4 and 5, one can see that the corresponding coke rate (m_{coke}) and direct reduction degree of iron (r_d) decrease when injected fuel rate ($m_{\text{fuel, injected}}$) increases. However, the downtrend of both direct reduction degree of iron (r_d) and coke rate (m_{coke}) with plastic injection is more obvious than that with pulverized coal injection. As a certain amount of carbon is replaced by the injected fuel, the coke rate (m_{coke}) with plastic injection or pulverized coal injection decreases. As part of hydrogen in the injected fuel takes part in direct reduction of iron (r_d), the direct reduction degree of iron (r_d) decreases. In

addition, as hydrogen content of plastic is higher than that of pulverized coal, the downtrend of direct reduction degree of iron (r_d) with plastic injection is more obvious than that with pulverized coal injection.

From Figures 2-5, one can see that plastic injection is more efficient in both coke conservation and decrease of direct reduction degree of iron (r_d) when the hydrogen content of plastic is higher than that of pulverized coal.

4.2.2 Influence of carbon-hydrogen mass ratio of plastic on optimization results

The carbon-hydrogen mass ratio of plastic ($n_{C/H,plastic}$) means the ratio of the mass of carbon to the mass of hydrogen in plastic. Figures 6 and 7 show the relationships among the minimum CO₂ emission (F_{min}), its corresponding direct reduction degree of iron (r_d), coke rate (m_{coke}) and the carbon-hydrogen mass ratio of plastic ($n_{C/H,plastic}$), respectively.

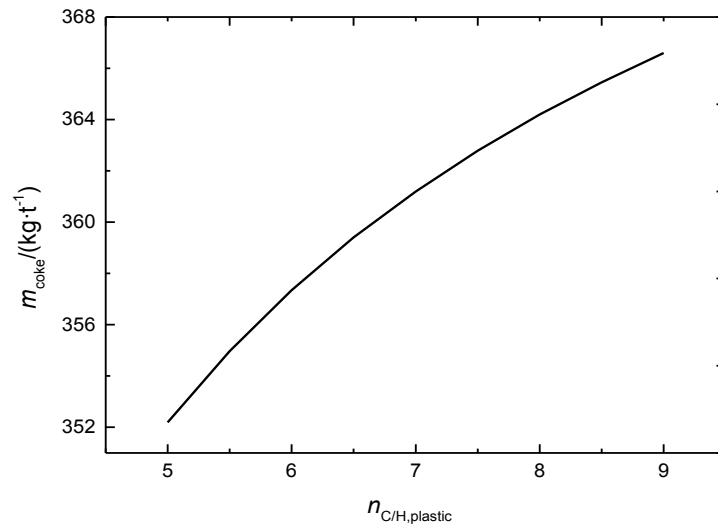


Figure 6. Coke rate (m_{coke}) versus carbon-hydrogen mass ratio of plastic ($n_{C/H,plastic}$) corresponding to the minimum CO₂ emission (F_{min})

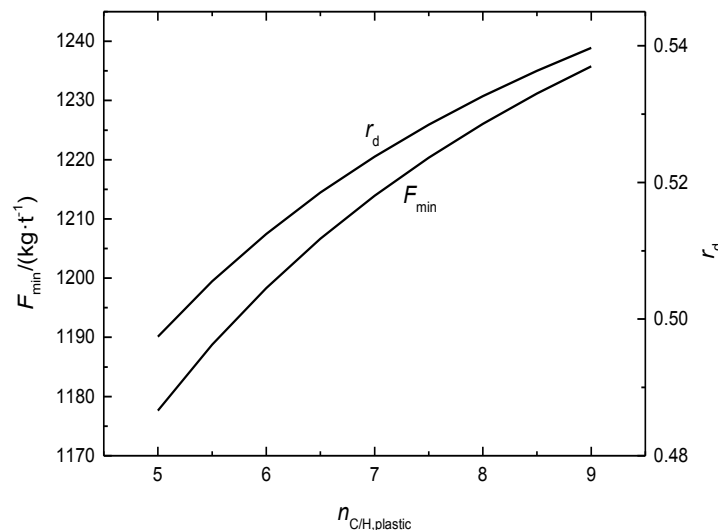


Figure 7. The minimum CO₂ emission (F_{min}) and the corresponding direct reduction degree of iron (r_d) versus carbon-hydrogen mass ratio of plastic ($n_{C/H,plastic}$)

Figure 6 shows that the coke rate (m_{coke}) corresponding to the minimum CO₂ emission (F_{min}) decreases with the decrease of carbon-hydrogen mass ratio of plastic ($n_{C/H,plastic}$). This is due to the fact that the mass

of hydrogen getting into blast furnace increases with the decreases of carbon-hydrogen mass ratio of plastic ($n_{C/H,plastic}$), as well as the mass of hydrogen involved in direct reduction of iron. As a result, the mass of carbon involved in direct reduction of iron (r_d) decreases. Thus, the coke rate (m_{coke}) decreases with the decrease of carbon-hydrogen mass ratio of plastic ($n_{C/H,plastic}$).

Figure 7 shows that both the minimum CO₂ emission (F_{min}) and its corresponding direct reduction degree of iron (r_d) decrease with the decrease of carbon-hydrogen mass ratio of plastic ($n_{C/H,plastic}$). As has been noted, coke rate decreases with the decrease of carbon-hydrogen mass ratio of plastic ($n_{C/H,plastic}$). The injected fuel rate ($m_{fuel,injected}$), however, is not changed. Therefore, both fuel rate (m_{fuel}) and carbon consumption decrease, and the minimum CO₂ emission (F_{min}) decreases. As a result of decreasing carbon-hydrogen mass ratio of plastic ($n_{C/H,plastic}$), the mass of hydrogen involved in reduction increases and the level of indirect reduction are improved. Thus, the direct reduction degree of iron (r_d) decreases. From Figures 6 and 7, one can conclude that injecting plastic with a low carbon-hydrogen mass ratio ($n_{C/H,plastic}$) is more beneficial to coke conservation, emission reduction and strengthening smelting than injecting plastic with a high carbon-hydrogen mass ratio ($n_{C/H,plastic}$).

4.2.3 Influences of blast parameters on optimization results

Figures 8-10 show the relationships among the minimum CO₂ emission (F_{min}) and its corresponding coke rate (m_{coke}), blast temperature (T_b), blast oxygen enrichment degree (f), and blast humidity (φ), respectively.

From Figure 8, one can see that the minimum CO₂ emission (F_{min}) and its corresponding coke rate (m_{coke}) decrease when blast temperature (T_b) increases. The calculations show that the minimum CO₂ emission (F_{min}) and its corresponding coke rate decrease about 3.35 kg/t-hot metal and 1.07 kg/t-hot metal, when blast temperature (T_b) increases about 10 °C. Figure 9 shows that both the minimum CO₂ emission (F_{min}) and its corresponding coke rate (m_{coke}) increase when blast oxygen enrichment degree (f) increases. Figure 10 shows that the minimum CO₂ emission (F_{min}) and its corresponding coke rate (m_{coke}) increase when blast humidity (φ) increases.

From Figures 8 and 10, one can conclude that the technology of improving blast temperature (T_b) or dehumidifying blast are beneficial for coke conservation and emission reduction. From Figure 9, one can conclude that blast oxygen enrichment degree (f) should be controlled within a proper range as emission can be increased by a high blast oxygen enrichment degree (f).

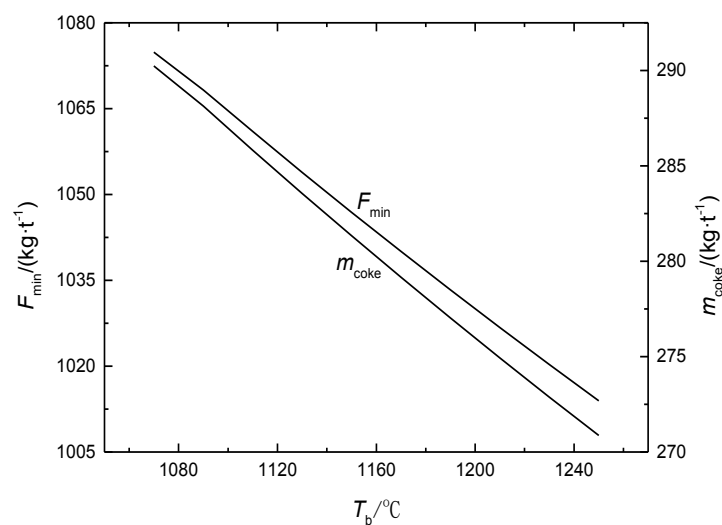


Figure 8. The minimum CO₂ emission (F_{min}) and the corresponding coke rate (m_{coke}) versus blast temperature (T_b)

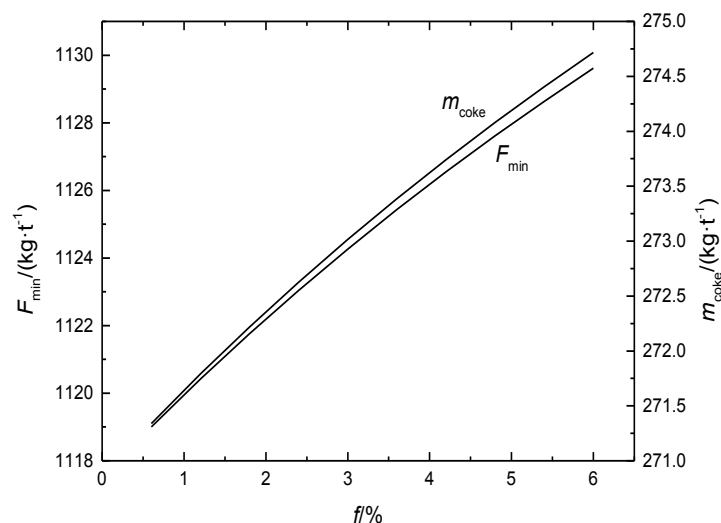


Figure 9. The minimum CO₂ emission (F_{\min}) and the corresponding coke rate (m_{coke}) versus blast oxygen enrichment degree (f)

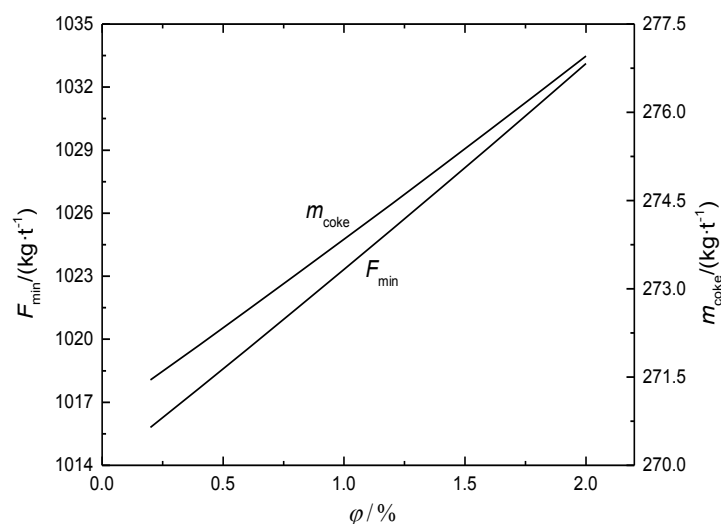


Figure 10. The minimum CO₂ emissions (F_{\min}) and the corresponding coke rate (m_{coke}) versus blast humidity (ϕ)

5. Conclusions

Base on material balance and energy balance of blast furnaces, an optimization model for blast furnace iron-making with the CO₂ emission reduction as optimization objective is established by using nonlinear programming method. The calculation program is compiled on the MATLAB, and the model is solved by using SQP algorithm in the optimization toolbox of the MATLAB. Comparative analyses for the effects of plastic injection and pulverized coal injection on the CO₂ emissions of the blast furnace are performed. The effects of carbon-hydrogen mass ratio of plastic, blast temperature, blast oxygen enrichment degree of blast and blast humidity on coke rate and direct reduction degree of iron are analyzed. The results show that plastic injection is beneficial for decreasing coke rate, fuel rate and direct reduction degree of iron when injecting plastic with a low carbon-hydrogen mass ratio. The CO₂ emission with plastic injection is less than that with pulverized coal injection. Plastic injection with a low carbon-hydrogen mass ratio can do more to decrease coke rate and emission.

Acknowledgments

This paper is supported by the National Key Basic Research and Development Program of China (973) (Project No. 2012CB720405).

References

- [1] Sen P K. CO₂ accounting and abatement: an approach for iron and steel industry. *J. Trans. Indian Inst. Met.*, 2013, 66(5-6): 711-721.
- [2] Sarker T, Coahan M. Energy sources and carbon emissions in the iron and steel industry sector in South Asia. *J. IJEEP*, 2013, 3(1): 30-42.
- [3] Kundak M, Lazic L, Crinko J. CO₂ emissions in the steel industry. *J. Metalurgija*, 2009, 3(48): 193-197.
- [4] Hasanbeigi A, Lynn K, Marlene A. *Emerging Energy-Efficiency and Carbon Dioxide Emissions-Reduction Technologies for the Iron and Steel Industry*. Berkeley: Lawrence Berkeley National Laboratory, 2013.
- [5] Ghanbari H, Helle M, Saxen H. Process integration of steelmaking and methanol production for decreasing CO₂ emissions - A study of different auxiliary fuels. *J. Chem. Eng. Processing*, 2012, 61: 58-68.
- [6] Ghosh A, Majumdar S K. Modeling blast furnace productivity using support vector machines. *J. Int. J. Adv. Manuf. Techno*, 2011, 52(9-12): 989-1003.
- [7] Gao C H, Zhou Z M, Chen J M. Assessing the predictability for blast furnace system through nonlinear time series analysis. *J. Ind. Eng. Chem. Res.*, 2008, 47(9): 3037-3045.
- [8] Hussain M M. *Ore Reduction Kinetics and Simulation of a Lead Blast Furnace*. The University of New Brunswick, 1987.
- [9] Chu M. *Study on super high efficiency operations of blast furnace based on multi-fluid model*. D. Sendai: Tohoku University, 2004.
- [10] Han Y H, Wang J S, Lan R Z. Kinetic analysis of iron oxide reduction in top gas recycling oxygen blast furnace. *J. Iron-making and Steelmaking*, 2012, 39(5): 313-317.
- [11] Rasul M G, Tanty B S, Mohanty B. Modeling and analysis of blast furnace performance for efficient utilization of energy. *Appl. Therm. Eng.*, 2007, 27(1): 78-88.
- [12] Emre E M, Gürgen S. Energy balance analysis for Erdemir blast furnace number one. *Appl. Therm. Eng.*, 2006, 26(11-12): 1139-1148.
- [13] Ziebig A, Stanek W. Energy and exergy system analysis of thermal improvements of blast-furnace plants. *Int. J. Energy Res.*, 2006, 30(2): 101-114.
- [14] Ziebig A, Lampert K, Szega M. Energy analysis of a blast-furnace system operating with the Corex process and CO₂ removal. *Energy*, 2008, 33(2): 199-205.
- [15] Helle H, Helle M, Saxen H. Mathematical optimization of iron-making with biomass as auxiliary reductant in the blast furnace. *ISIJ Int.*, 2009, 49(9): 1316-1324.
- [16] Helle H, Helle M, Saxen H. Nonlinear optimization of steel production using traditional and novel blast furnace operation strategies. *Chem. Eng. Sci.*, 2011, 66(24): 6470-6481.
- [17] Yang T J, Gao B, Lu H S. Optimization aimed at the lowest coke consumption by model and analysis of the application. *J. University. Sci. Techn. Beijing*, 2001, 23(4): 305-307 (in Chinese).
- [18] Zhang Q, Yao T, Cai J, Shen M. On the multi-objective optimal model of blast furnace iron-making process and its application. *J. Northeastern(Nature Sci.)*, 2011, 32(2): 270-273 (in Chinese).
- [19] Minoru A, Tasturo A, Michitaka S. Development of waste plastics injection process in blast furnace. *ISIJ. Int.*, 2000, 40(3): 244-251.
- [20] Dongsu K, Sunghye S, Seungman S. Waste plastics as supplemental fuel in the blast furnace process: improving combustion efficiencies. *J. Hazard. Mater.*, 2002, 94(3): 213-222.
- [21] Minoru A, Masahiko K, Hidekazu T. Evaluation of waste plastics particle for blast furnace injection. *J. Japan Inst. Energy*, 2012, 91(2): 127-133.
- [22] Biswas A K. *Principles of blast furnace iron-making: Theory and practice*. Brisbane: Cootha, 1981.
- [23] Kieatv B I, Yaroshenko Y G, Suchkov V D. *Heat Exchange in Shaft Furnace*. Oxford: Pergamon Press, 1967.
- [24] Ding J, Gao B, Wang S, Zhang Q. Effect of silicon content in molten iron on carbon emission in blast furnace. *J. Res. Iron Steel*, 2011, 39(5): 1-3 (in Chinese).
- [25] Na S R. *Differentiation and Analyses of Iron-Making Calculations*. Beijing: Metallurgical Industry Press, 2010 (in Chinese).
- [26] Wang S L. *Metallurgy of Iron and Steel (Iron-Making Part)*. Beijing: Metallurgical Industry Press, 2013 (in Chinese).

- [27] Venkataraman P. Applied Optimization with MATLAB Programming (2nd ed.). Hoboken: John Wiley & Sons, Inc., 2009.
- [28] Zhu Z B, Zhang K C. A new SQP method of feasible directions for nonlinear programming. Appl. Math. Comput., 2004(148): 121-134.



Xiong Liu received his BS Degree in 2011 from the Changsha University of Science and Technology and his MS Degree in 2013 from the Naval University of Engineering, P R China. He is pursuing for his PhD Degree in power engineering and engineering thermophysics from Naval University of Engineering, P R China. His work covers topics in engineering thermodynamics and optimization for iron and steel process. Dr Liu is the author or coauthor of 4 peer-refereed articles.



Xiaoyong Qin received all his degrees (BS, 2000; PhD, 2005) in power engineering and engineering thermophysics from the Naval University of Engineering, P R China. His work covers topics in finite time thermodynamics, technology support for propulsion plants and optimization for iron and steel process. Associate Professor Qin is the author or coauthor of over 40 peer-refereed articles (over 20 in English journals).



Linggen Chen received all his degrees (BS, 1983; MS, 1986, PhD, 1998) in power engineering engineering thermophysics from the Naval University of Engineering, P R China. His work covers diversity of topics in engineering thermodynamics, constructal theory, turbomachinery, reliability engineering, technology support for propulsion plants and optimization for iron and steel process. He been the Director of the Department of Nuclear Energy Science and Engineering, the Superintendent of Postgraduate School, and the President of the College of Naval Architecture and Power. Now, he is Direct, Institute of Thermal Science and Power Engineering, the Director, Military Key Laboratory Naval Ship Power Engineering, and the President of the College of Power Engineering, Naval University of Engineering, P R China. Professor Chen is the author or co-author of over 1430 peer-refereed articles (635 in English journals) and nine books (two in English).

E-mail address: lgchenna@yahoo.com; linggenchen@hotmail.com, Fax: 0086-27-83638709 Tel: 0086-27-83615046



Fengrui Sun received his BS Degrees in 1958 in Power Engineering from the Harbing University of Technology, P R China. His work covers a diversity of topics in engineering thermodynamics, constructal theory, reliability engineering, and marine nuclear reactor engineering. He is a Professor in the College of Power Engineering, Naval University of Engineering, P R China. Professor Sun is the author or co-author of over 850 peer-refereed papers (over 440 in English) and two books (one in English)